Journal of
Ceramic Science
and Technology

J. Ceram. Sci. Tech., **05** [02] 137-144 (2014)
DOI: 10.4416/JCST2013-00040
available online at: http://www.ceramic-science.com
© 2014 Göller Verlag

Manufacture of Rotationally Symmetric Multilayer Refractory Devices for Steel Casting Applications by Spiral Winding of Ceramic Green Tapes

D. Jakobsen*[1], R. Hammerbacher[1], S. Dudczig[2], T. Fey[1], A. Roosen[1]

[1]University of Erlangen-Nuremberg, Department of Materials Science, Glass and Ceramics, D-91058 Erlangen, Germany
[2]Technische Universität Bergakademie Freiberg, Institute of Ceramics, Glass and Construction Materials, D-09599 Freiberg, Germany

received Nov 11, 2013; received in revised form Jan 22, 2014; accepted Mar 21, 2014

Abstract

In order to create rotationally symmetric refractory devices from ceramic green tapes, the spiral winding method, which is mainly known from the paper industry, was applied. Different green tapes with varying properties with regard to shrinkage, porosity and Young's modulus were used to generate multilayer tubes with the spiral winding and the cold low pressure lamination technique. The tubes were fired in air and their microstructure was investigated. Thermal shock tests were conducted to evaluate the applicability of the fabricated structures for refractory applications. The correlation between the microstructure and thermal shock behaviour of the tubes is discussed.

Keywords: Spiral winding, green tapes, refractories, thermal shock

I. Introduction

The reduction of greenhouse gas emissions has become a major issue in almost every technical and industrial field. Many commercial refractories are carbon-bound, and thus release CO and CO_2 gases during the steelmaking process [1,2]. Therefore, substituting carbon-free raw materials for the carbon-bound ones is very interesting in terms of "clean steel technology". However, the absence of carbon also involves a decline in thermal shock and corrosion resistance [1]. Therefore, the development of advanced refractories to compensate for this disadvantage is of great interest. Ceramic multilayer technology, which is based on cast green tapes, has the potential to generate such advanced structures [3,4]. The technique of multilayer composites allows the generation of structures with improved mechanical and thermal properties [5,6]. One concept is based on combining different layers exhibiting different shrinkage behavior and/or coefficients of thermal expansion (CTE) in order to generate internal stresses which could counteract the thermal stresses resulting from thermal shock. Another way, which is the goal of this work, is based on the generation of weak bonds at interfaces, which was described in literature as yielding excellent thermal shock behaviour [7]. Regardless of which method is employed, the use of the green tape multilayer technology for refractory applications generally requires the ability to manufacture rotation-symmetric devices from green tapes; it is obvious to use winding as a manufacturing technique for such devices.

* Corresponding author: daniel.jakobsen@ww.uni-erlangen.de

Winding is a well-known technology in different applications, e.g. winding of thermoplastics, inductors, or superconductors [8–10]. Depending on the direction of the winding axis relative to the direction in which the material is moved, a distinction is generally made between parallel, vertical and spiral winding. As the axis of rotation, a core or a mandrel may be used [11]. Offering the possibility of endless winding, spiral winding is the most widespread method. This technique is often used in the paper industry to fabricate devices, like paper rolls [12–14]. Reports about winding ceramic green tapes are rare, but there have been attempts to fabricate some structures, such as piezoelectric multilayer actuators in the shape of a double helix structure [15]. Spiral winding of ceramic green tapes was conducted by Scheithauer *et al.* using zirconia and calcium aluminate tapes to manufacture tubes for energy, environmental, and high-temperature applications [16]. Götschel *et al.* combined the winding of preceramic papers and ceramic green tapes to prepare a rotation-symmetric structure for refractory applications [17]. They used the non-continuous parallel winding technique and a cold low pressure lamination technique and obtained crack-free structures after firing. However, in parallel winding, the length of the tube is limited by the width of the green tape. To lengthen the wound tube, a second winding step has to be started next to the first one. This interface is a weak point in the green body and will probably cause cracking during firing.

To avoid this disadvantage, the applicability of the spiral winding process to ceramic green tapes will be demonstrated in this study as a continuous method to manufacture rotation-symmetric nozzles for steel casting ap-

plications. Dense- and porous-sintering green tapes made of alumina and spinel were used. The fired samples were characterized with regard to their sintering, microstructure and thermal shock behavior.

II. Experimental Procedure

Fine- (d_{50}: 1 – 3 μm) and coarse-grained (d_{max} < 45 μm) alumina and spinel powders were used to prepare slurries for the casting of green tapes. The slurries were based on organic solvents; their preparation was described by Götschel *et al.* [4]. The tape compositions used in the present paper are listed in Table 1. The deagglomerated and homogenized slurries were exposed to an underpressure of 230 mbar for 20 min in order to remove air bubbles under slow rotation. The slurries were poured into a double-chamber casting head and cast with blade gaps of 1500 μm and 2500 μm, resulting in dried green tapes with thicknesses of around 600 μm and 1200 μm, respectively. After drying of the tapes, square samples of the thinner tapes with a dimension of 27.5 x 27.5 mm² and strips with a length of 30 mm and a width between 10 and 30 mm were cut with a hot knife (Groz-Beckert KG, Albstadt, Germany) at a temperature of 60 °C. The square samples were fired in air at 1700 °C for 5 h (HT 16/17, Nabertherm, Lilienthal, Germany) and characterised concerning shrinkage by measuring the geometry before and after sintering. Green and sintered density as well as porosity after firing were determined using an Archimedes method according to EN 623 – 2 [18]. The coefficient of thermal expansion was determined by means of a dilatometer (DIL 402C, Netzsch, Selb, Germany) using a sintered piece with the dimensions 5 x 20 mm². The dynamic Young's modulus was determined by means of an ultrasonic impulse reflection method (USD10, Krautkrämer, Germany) according to EN 843 – 2 [19] using the sintered square samples. The bending strength of the fired tapes was investigated in double-ring flexural tests according to DIN 51105 using the square-shaped specimens which were already used for previous characterisation. Twenty specimens of each composition were measured with a constant loading speed of 1.0 mm/min using a universal testing machine (Instron Model 4204, Instron Wolpert, Germany). For calculation of the characteristic strength σ_0 and the Weibull modulus m, the Likelihood method was applied.

Table 1: Compositions of the investigated green tapes (A: Alumina; S: Spinel).

Tape	Fine powder fraction [wt%]	Coarse powder fraction [wt%]
A1	100	-
A2	45	55
A3	15	85
S1	100	-
S2	15	85

To measure the minimum bending radius of each investigated tape, a method developed by Feilhauer [20] was used. A strip of the corresponding green tape of the dimensions 200 x 10 mm² was inserted between the outside jaws of a vernier caliper, and, subsequently, the jaws were closed carefully until cracks became visible in the tape. At that point, the half-length value of the caliper was interpreted as the minimum bending radius of the tape. This method was applied at room temperature and after heating the strips up to 60 °C.

For spiral winding, suitable tapes were cut to strips of 200 mm in length. Their width was varied in steps of 2.5 mm from 10 mm up to 30 mm. The strips were rolled up manually on a mandrel with a diameter of 4 mm and a length of 250 mm. To facilitate the removal of the tube after winding, the mandrel was covered with a non-adhesive polymer film. To join the tapes directly during the winding process, cold low pressure lamination was used [17,21]. For that purpose, an aqueous dispersion of copolymerized polyvinyl acetate was applied on the upper side of each tape strip as an adhesive. Winding of one layer was done edge-to-edge without any overlap of the tape. As the used tape strips had a constant length, their width had to be increased layer-wise due to higher material needs as the circumference of the winding axis increases. Starting with the strip with the lowest width of 10 mm, it was increased for each new layer by 2.5 mm. Each layer was displaced by 90° to the previous one, according to the scheme in Fig. 1, and wound tightly to get a good joining and to limit the defect size. In order to be able to mount the tube in a testing device, a fixture consisting of A1-tape strips with a green thickness of 600 μm was additionally wound on one end of the nozzle using the parallel winding technique. A sintered nozzle with a fixture is shown in Fig. 2. The strain ε which occurs at the outside of the tape can be calculated for each wound layer according to Equation 1, with the thickness d of the wound layer and the radius r_0, which is the sum of the radius of the mandrel and the thickness of all already wound layers underneath [15].

Fig. 1: Scheme of the spiral winding technique (dark: first layer; light: second layer, rotated by 90° to the previous layer).

Fig. 2: Sintered nozzle with a fixture after removal of the outer layer (tube length: ~ 80 mm).

$$\varepsilon = \frac{r_0 + d}{r_0} - 1 \qquad (1)$$

For preliminary tests, simple structures of A1-tapes were wound starting with a single-layer tube, building up to ten layers. For multilayer composite assemblies, green tapes of

the two materials were combined. All wound tubes were removed from the mandrel and sintered in air at 1700 °C for 5 h. Due to the high amount of organic components, all multilayer structures had to be debinded slowly at a heating rate of 15 K/h up to 500 °C. Beyond this point, a heating rate of 5 K/min was used. During firing, the horizontally positioned tubes were supported by setter plates. In order to avoid friction between the setter material and the samples, a green tape identical with the outermost layer of the tube was inserted in between.

The microstructure of the fired nozzles was visualized by means of scanning electron microscopy (SEM) and micro tomography (μ-CT). For these purposes, the nozzles were embedded in an epoxy resin, which was cured and de-aired under vacuum. The tubes were cut into segments with a diamond saw, polished, and coated with a thin gold layer. Micrographs of the samples were taken using an SEM (Quanta 200, FEI, Eindhoven, the Netherlands) at a magnification of 39 and 400, respectively, by detection of backscattered electrons at an accelerating voltage of 20 kV.

Additionally, one inner segment was examined with high-resolution X-ray micro tomography using a Skyscan 1172 (Skyscan B.V., Kontich, Belgium) with an 11-megapixel detector. The X-ray tube (tungsten target) was operated at a voltage of 80 kV and a current of 100 μA using an additional Al/Cu filter. The scan was performed with a rotation step of 0.25° over 360°, random movement of 10, with a resolution of 4.75 μm/pixel. Measured raw data sinograms were reconstructed with the tomographic reconstruction software (NRecon Client and Server 1.6.9 with GPU support, Skyscan, Kontich, Belgium), which calculates the two-dimensional (2D) cross-sections after adjusting grey value levels. The 3D visual images and STL models were generated using imaging software (Amira 5.4.5, Visage Imaging, Berlin, Germany) after labeling with a global threshold and using a 26-side growing algorithm on all layers.

To estimate the thermal shock behaviour, tests with a tin melt (T: 500 °C), an aluminum melt (T: 800 °C, 900 °C and 1000 °C) and a steel melt (T: 1645 °C) were conducted. For the test in molten tin, the samples were dipped completely into the liquid by means of a high-temperature stable metallic wire. After cooling down to room temperature, the samples were shocked again, up to eight times. For higher temperature differences, an aluminum melt was used which was placed in an oven at 800, 900 and 1000 °C, respectively. Outside the oven, the samples were inserted into a fixture and then quickly dipped into the liquid metal. In each case, the specimens were kept in the liquid for one minute. The tubes were removed and cooled down to room temperature in air and the thermal shock was repeated. For testing the applicability of the nozzles under realistic ambient conditions of use, one tube was inserted into the fixture of a steel casting simulator. The functionality of this simulator is described in the literature [22]. Rotating at 30 rpm, the nozzle was dipped into a steel melt (42CrMo4) at 1645 °C for 30 s without pre-heating. The tube with an overall length of around 80 mm was submerged into the liquid metal to about the half of its length. At the end of the test, the tube was removed out of the melt and quenched in the ambient air.

After exposure to thermal shock by these different techniques, the tubes were cut into rings with a diamond saw. The rings were coloured by being dipped into a fuchsine solution in order to visualize cracks and delamination. Images of the rings were taken with a photo camera.

III. Results and Discussion

(1) Bending radius

The flexibility of the green tapes is provided by a binder/plasticizer mixture during slurry preparation [4]; the ratio of this mixture determines its glass transition temperature T_g and was kept constant for all tapes. The amount of this polymer mixture was between 5 and 7.5 wt% referring to the solid content. The amount of organic additives was chosen to be as low as possible, but high enough to avoid drying cracks in the green tape.

Fig. 3 shows the results of the bending tests. It is demonstrated that the flexibility of the tapes differs to a large extent. The dashed line represents the radius of the mandrel used for winding. Only tapes A1 and S1 exhibit acceptable bending behaviour. These tapes consist solely of powders with a d_{50} of 1 – 3 μm. The thicker A1 tape (green tape thickness ≈ 1200 μm, the other tapes had a thickness of approximately 600 μm) cannot be bent as much as the thinner A1 tape; therefore tapes suitable for winding are limited in thickness. The other tapes with insufficient bending behaviour contain specific amounts of coarse powder (see Table 1), resulting in larger inhomogeneities in the green tape microstructure of these so-called bimodal tapes. Comparing the bimodal tapes with identical coarse-grain fraction (A3 and S2), spinel shows a slightly lower bending radius compared to the alumina tape. Pre-heating to 60 °C improves the flexibility of all tapes significantly. It is recognizable that pre-heating is necessary for winding of the inner layers of the rotation-symmetric structures. For the outer layers, pre-heating is not necessary due to the increase in bending radius. The maximum strain that layer S1 can resist is 40.5 % at room temperature and 75 % at 60 °C, inserting the measured smallest bending radius (see Fig. 3) in Equation 1. Applying the radius of the mandrel (2 mm), a strain of 30 % occurs in this layer, which is not critical. As the number of layers increases, the strain in the tapes during winding decreases. These results were all taken into account for the following experiments.

(2) Sintering shrinkage and properties of the sintered tapes

According to results of an earlier publication, the porosity and sintering shrinkage can be adjusted to a certain extent with the addition of specific amounts of coarse particles to the finer powder fraction [4]. Tapes derived from fine-grained powders, i.e. A1 and S1, exhibit a sintered density of 96 to 98 % TD. The lower specific surface area of the coarse particles results in a lower driving force for densification, which leads to reduced shrinkage and therefore higher porosity and simultaneously lower density starting from an almost identical green density (Fig. 4, Table 2). It has to be taken into account that lamination of these green tapes causes a certain pre-densification of the green tape microstructure; therefore, the resulting shrink-

age and porosity of multilayer components are lower compared to single tapes of similar composition [4]. The Young's modulus and the bending strength of the fired tapes also depend on the porosity (Table 3). Values of the modulus of elasticity between 130 and 400 GPa were achieved, whereas the characteristic bending strength ranged between 100 and 350 MPa.

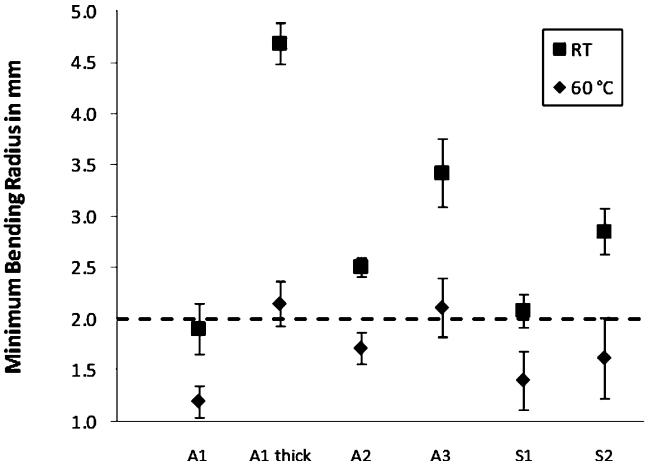

Fig. 3 : Minimum bending radius of the investigated tapes at room temperature and 60 °C; dashed line: radius of the winding mandrel.

Due to the different densification behaviour, the shrinkage of the green tapes differs a lot, too. The dense tapes exhibit a linear sintering shrinkage between 17 and 20 %, whereas tapes composed of bimodal powder mixtures show shrinkage values of 8 to 14 %, depending on the amount of coarse particles. In the case of multilayer composite structures, these differences in shrinkage would cause stresses during sintering. In addition, the mismatch in thermal expansion between the investigated material systems (Table 3) would additionally influence thermal stresses. A prerequisite for the generation of internal stresses in the structure after cooling is a joint interface between such tapes; if the local stresses are too high, they are released by means of delamination. Because the CTE difference between the two materials used, alumina and spinel, is small (Table 1), stresses caused by CTE differences can be neglected. But stresses due to sintering mismatch can be used to form delaminated areas.

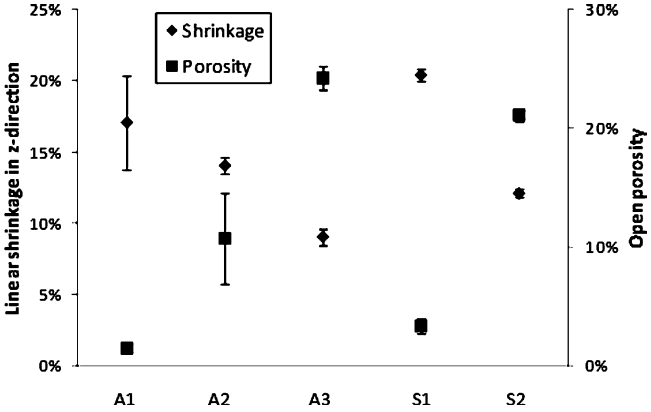

Fig. 4 : Linear sintering shrinkage in z-direction and open porosity of the investigated tapes.

(3) Monolithic multilayer structures

At first, monolithic multilayer structures were fabricated with just the monomodal alumina tape A1; thus, stresses due to shrinkage mismatch are minimized. After firing, the tubes made of wound tapes were evaluated with regard to crack formation and delamination behaviour in relation to the total number of layers.

Table 2: Green density, sintered density, and shrinkage characteristics of the investigated tapes.

Tape	Green density/%TD*	Sintered density/%TD*	Linear shrinkage x-direction/%	Linear shrinkage y-direction/%	Linear shrinkage z-direction/%
A1	60.8	98.5	17.2	17.4	17.1
A2	63.6	89.3	11.7	12.8	14.0
A3	63.3	75.8	8.0	8.5	9.0
S1	59.7	96.7	16.7	17.6	20.4
S2	62.1	78.9	9.7	10.3	12.1
* % of the theoretical density					

Table 3: Mechanical properties and thermal expansion data of the investigated tapes after firing.

Tape	Young's modulus/GPa	Characteristic strength/MPa	Weibull modulus	$CTE_{600-1500\,°C}/10^{-6}\ K^{-1}$
A1	409	352	5.3	10.2
A2	263	161	7.0	
A3	149	120	5.2	
S1	264	200	7.8	10.0
S2	132	103	8.2	

It was observed that a single spiral wound layer does not keep its shape after removal of the mandrel (Fig. 5). As a result, the coiled one-layer tube widened during sintering; the contact between the tape edges was not strong enough to keep the wound structure together. Additionally, the sintered tube was slightly flattened. With the addition of a second and third layer, each wound perpendicular to the previous one (see Fig. 1), widening or flattening of the samples during sintering could be prevented (see Fig. 5). The samples were crack-free and slight delamination only occurred at the ends of the tubes. This means that the 90° displacement of the winding strengthened the joint between the single tapes in the green state and during firing. Winding of four or more layers seems to generate high stresses during binder burnout and sintering, which exceed the strength of the joined ceramic tapes and result in crack formation in the outer layers during thermal treatment (see Fig. 5). These cracks occurred even though the tubes were crack-free in the green state. The most likely explanation for this phenomenon is the limited heat transfer from the outer layers to the inner ones. If the number of layers is small, the temperature gradient is low, and the outer layers do not exhibit any cracks. As the layer count increases, the temperature gradient increases. Therefore, cracking occurs in the outer layers because the earlier shrinkage onset of the outer layer compared to that of the inner layers results in stresses that exceed the strength of the material. During the proceeding sintering process, the cracked parts of the outer layers lift off from the core part of the tube, while the inner surface of the innermost layer does not crack. This lift-off occurs because the bond between the laminated tapes is not strong enough. In the inner part of the tube, some delamination, warpage effects, and crack formation occurred during firing. This can be ascribed to the spiral winding process, which results in partially incomplete contact between the tape currently being wound and the mandrel or the previously wound coils, respectively. This will cause a small bulge in the wound tapes for each following layer and ultimately causes the defects in the microstructure described above.

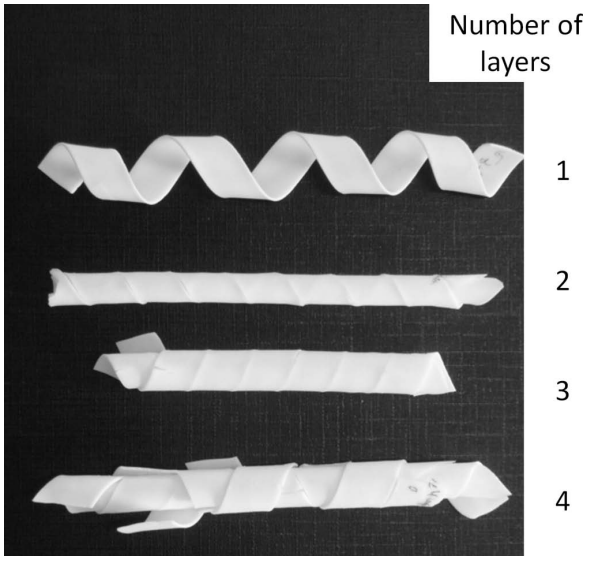

Fig. 5: Sintered monolithic multilayer tubes with increasing number of A1-layers.

(4) Multilayer composite structures

To improve the thermal shock resistance parameter R, tapes with higher porosity and therefore lower Young's modulus were used. In order to avoid infiltration by a steel slag, dense-sintering layers were generally used for the inner layers of the tubes. By combining tapes with different shrinkage behavior, it was possible to generate structures with moderate delamination in the micro- and macroscopic scale, which still offered enough contact points between the individual tapes to keep them together.

It was found that the tape sequence S1-S1-S1-S2-S2-A3-A3-A2-A2-A1 resulted in almost crack-free structures with the desired delamination behavior, but the delaminations had an inhomogeneous distribution. Again, the dense-sintering outermost layer exhibited cracks and lifted off the tube in all experiments, whereas the subjacent layers held together. Therefore, this outermost layer was applied as a sacrificial layer and was removed after the heat treatment. A complete, sintered nozzle of the given tape sequence with a parallel wound fixture is depicted in Fig. 2.

Regarding the SEM overview image (see Fig. 6), it is obvious that every interface contains delamination to some extent. The biggest delamination of a few mm in length can be seen at the interface between the dense-sintering S1 and porous S2 layers. The shrinkage difference of these two tape systems is so high that they remain in contact at only some points of the bottom position, which is not located in the image. Additionally, there are also some vertical gaps which do not have their origin in cracking during firing. These are the positions where the edges of the tape windings (see Fig. 1) were in contact with each other in the green state, leaving a gap during shrinkage.

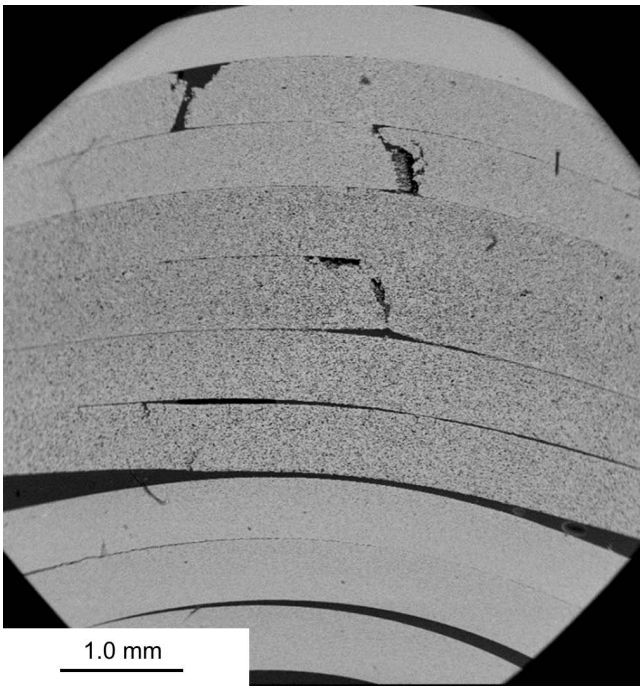

Fig. 6: SEM micrograph of a fired and unshocked nozzle segment; several delaminations between the single layers can be seen. Interruptions in upper layers occur at the contact line between two windings of one tape (see Fig. 1).

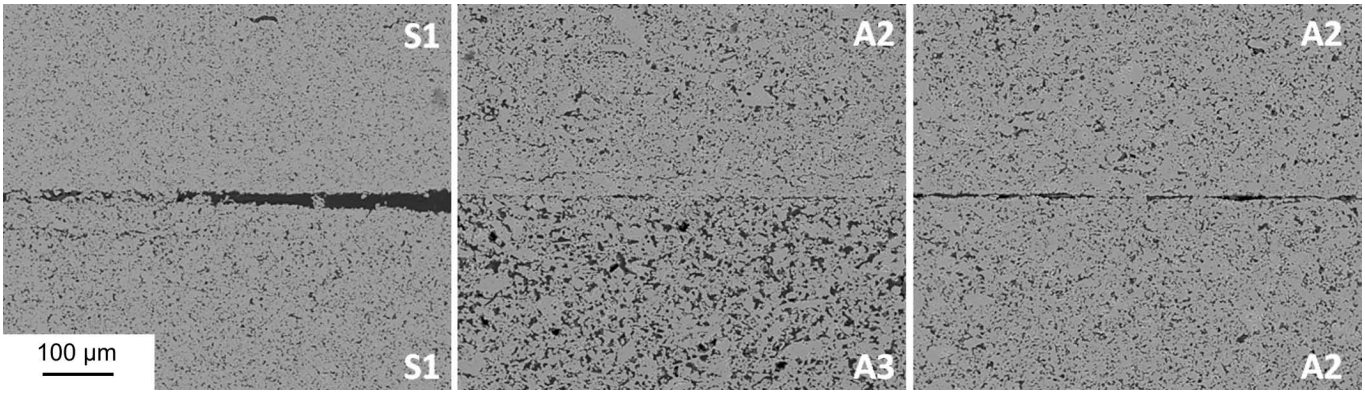

Fig. 7: SEM micrographs of several interfaces showing partial delamination and joined areas.

The higher resolution of the interfaces (Fig. 7) shows that the interfaces between the tapes also exhibit microscopic delaminations which are interrupted by joint parts. These defects have a magnitude of around 10 µm. Their origin is on the one hand based on shrinkage differences between different types of tapes and on the other hand also on the quality of lamination. There are no meshing effects like in planar multilayer structures that have been laminated by means of thermo compression. Therefore, small delaminations occur, even between equal tapes. The reconstruction of a tube segment from the µ-CT data with a slightly delaminated interface revealed that the cavities found at the interface are locally restricted phenomena (Fig. 8). There are enough contact areas thanks to the spiral wound multilayer structure that the tubes retain sufficient strength.

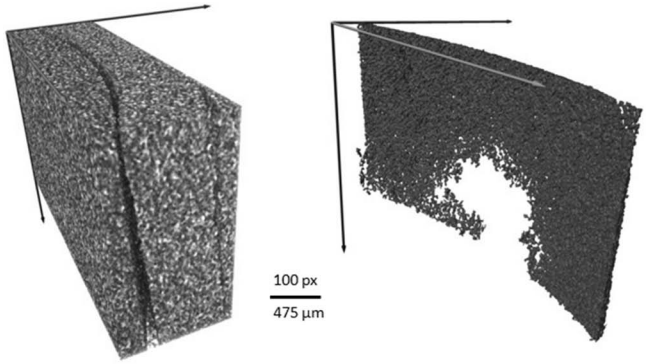

Fig. 8: 3-dimensional reconstruction of an interface between identical tape layers; left: material matrix, right: visualisation of the delamination zone.

This tube assembly, with its high defect concentration, was expected to be suitable to exhibit improved thermal shock behaviour. Therefore, these tubes were chosen for further characterisation regarding thermal shock. In all cases, the cracked outer layer was completely removed manually after firing, as mentioned above.

(5) Thermal shock tests

All samples endured multiple shocks up to eight times in 500 °C hot molten tin without any severe damage (Fig. 9). Multiple shocking up to eight times provoked slight cracks in the outer layer, but in the inner ones, no structural changes could be observed (Fig. 10). All cracks were perpendicular to the length axis of the wound strips and released stresses. After fivefold shock, small amounts of tin residue were found inside some inner cavities.

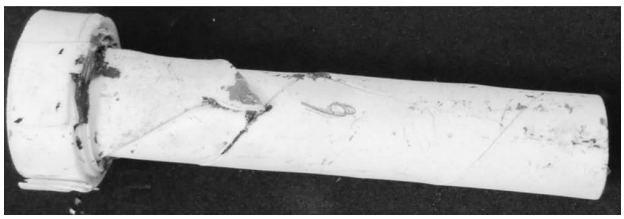

Fig. 9: Complete nozzle after six thermal shocks in tin melt (500 °C); all visible cracks were already formed during sintering.

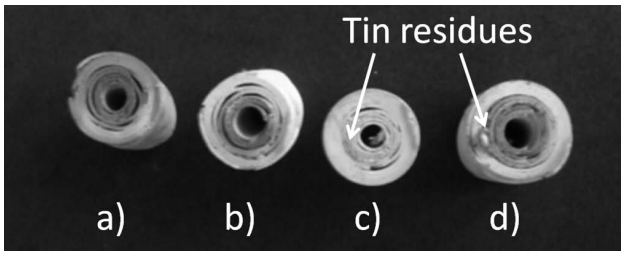

Fig. 10: Inner sections of sintered tubes after thermal shock into 500 °C hot tin melt; a) unshocked, b) one shock, c) five shocks, d) eight shocks; tin residues are incorporated in cavities after five or more shocks.

Using an aluminum melt, the tubes survived two shocks with barely any visible damage except some slight cracks in the outer layer at shock temperatures of 800 and 900 °C (Fig. 11). Shocking the samples at 1000 °C did not lead to severe damage either, but during sawing, a loss in strength was noticed which can be ascribed to additional formation of cracks in the inner regions of the tube caused by dipping into the liquid aluminum at 1000 °C. However, before sawing, the tube structure still holds together as one part without any loss of material; this is due to the spiral wound structure, which still offers enough contact areas between the wound tape layers to maintain structural integrity.

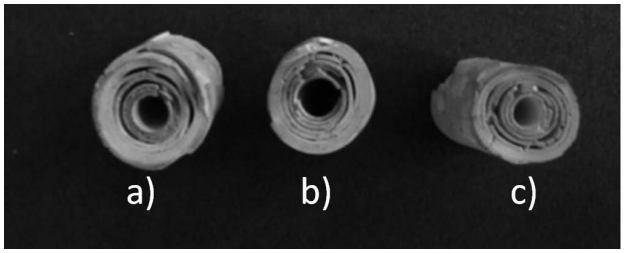

Fig. 11: Inner sections of sintered tubes after two thermal shock cycles in aluminum melt with a temperature of a) 800 °C, b) 900 °C, c) 1000 °C.

In the steel casting simulator, the tube endured the thermal shock and the test conditions in molten steel with a temperature of 1645 °C. After the removal of the nozzle from the hot steel melt of the steel simulator, the second thermal shock occurred. Some parts of the three outer layers broke off from the sample shortly after removal from the melt as a result of quenching in the ambient air. Even if this thermal cooling shock weakened the strength of the tube, its functionality is still present (see Fig. 12).

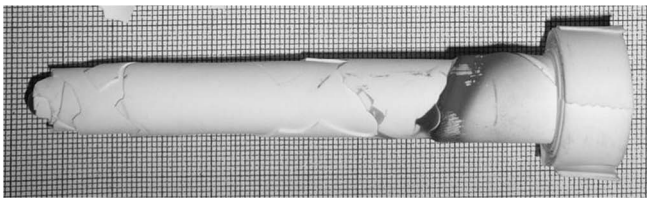

Fig. 12: Nozzle after dipping into steel melt (T: 1645 °C); outer layers are broken off, but the tube is still usable.

The conducted thermal shock tests are not sufficient to make any final conclusion about the performance of such wound multilayer refractory structures, but the results show that the tubes can resist temperature differences up to at least 1500 °C. The critical temperature difference for crack generation and propagation for these systems can be located between 900 and 1000 °C according to the definition of Hasselman [23], but these cracks do not cause catastrophic failure of the tubes. Even though the initial structure of the tubes is not homogeneous, the internal, but locally restricted delaminations and cracks result in an excellent thermal cycling capability. The defects, present in high concentration between the layers, intercept the stresses formed during thermal shock and preserve the entire structure from catastrophic failure. This is facilitated by the alternating use of relatively thin layers of high and low Young's modulus. Based on these results, future developments will be targeted at the controlled manufacture of such wound microstructures high in defects.

IV. Conclusions

The applicability of the spiral winding process of ceramic green tapes to manufacture rotationally symmetric devices like tubes and nozzles was demonstrated. For winding, pre-heating of the tape strips to 60 °C was necessary to increase their flexibility. Incrementally increasing the layer count in samples of fine-grained alumina tapes showed that only tubes that had up to three layers can be sintered crack-free. To achieve tubes with higher layer counts up to ten layers, the outer layers were composed of coarse-grained tapes with lower sintering shrinkage and with an outermost closing layer of a dense-sintering tape. Assemblies of ten layers have been manufactured in that manner. A closer investigation of the sintered tubes by means of SEM and micro tomography revealed that they contain the intended delaminations in micro- and macroscopic dimensions between joined areas, implying that the wound structure keeps the layers together as one part. These local defects were caused by sintering stresses in combination with weak bonding between the laminated green tapes.

Preliminary thermal shock tests have been conducted with ten-layer tubes consisting of dense-sintering spinel tapes in the inside followed by porous-sintering spinel and alumina tapes. The dense-sintering layer at the outside, which cracked during thermal treatment, was removed after sintering. It was found that several thermal shock cycles in 500 °C hot tin melt and in liquid aluminum at 800 and 900 °C caused minor crack formation, but no relevant structural changes occurred, whereas a thermal shock of 1000 °C caused a certain decline in strength, but again without leading to failure. A temperature difference of around 1600 °C caused damage in the outer layers and the nozzle became more fragile. In all cases, the tubes survived the shock without catastrophic failure. As the manufactured, unshocked structures showed locally restricted delaminations between the layers, it can be concluded that this defect structure is the reason for the good thermal shock behaviour and thermal cycling capability. Future work will focus on the controlled manufacture of such defect structures.

Acknowledgements

The authors wish to thank the German Research Foundation (Deutsche Forschungsgemeinschaft DFG, Priority Program SPP 1418 "FIRE", contract number RO 653/13 – 2) for its financial support and all members of the FIRE Group, especially C.G. Aneziris, for fruitful discussions.

References

1 Buhr, A.: Refractories for steel secondary metallurgy, *CN-Refractories*, **6,** [3], 19 – 30, (1999).

2 Aneziris, C.G., Jin, S.L., Li, Y.W., Roungos, V.: Interactions of carbon nanotubes in Al_2O_3-C Refractories for Sliding Gate Applications, Proceedings of the Unified International Technical Conference on Refractories, Salvador, Brazil, October 13 – 16, (2009).

3 Roosen, A.: Tape casting of ceramic green tapes for multilayer device processing, *Ceram.Trans.*, **97**, 103 – 121, (1999).

4 Götschel, I., Hayashi, Y., Kakimoto, K.-I., Roosen, A.: Tape casting of Al_2O_3, MgO, and $MgAl_2O_4$ for the manufacture of multilayer composites for refractory applications, *Int. J. Appl. Ceram. Tec.*, **9**, [2], 329 – 340, (2012).

5 Green, D.J., Cai, P.Z., Messing, G.L.: Residual stresses in alumina-zirconia laminates, *J. Eur. Ceram. Soc.*, **19**, [13 – 14], 2511 – 2517, (1999).

6 Danzer, R., Bermejo, R.: Failure resistance optimisation in layered ceramics desgined with strong interfaces, *J. Ceram. Sci. Tech.*, **1,** [1], 15 – 20, (2010).

7 Li, Z., Liu, J., Li, S., Du, H.: Microstructure, mechanical properties and thermal shock resistance of $LaPO_4$-ZrO_2, *J. Alloy. Compd.*, **480**, [2], 863 – 866, (2009).

8 Åström, B.T., Pipes, R.B.: Thermoplastic filament winding with on-line impregnation, *J. Thermoplast. Compos.*, **3**, 314 – 324, (1990).

9 Kitaguchi, H., Kumakura, H., Hayashi, T., Fujino, K.: A Bi-2223 layer-winding coil using 540 m tape including a joint inside the winding, *IEEE T. Appl. Supercon.*, **21,** [3], 1624 – 1627, (2011)

10 Qiu, J., Hanson, A.J., Sullivan, C.R.: Design of toroidal inductors with multiple parallel foil windings, 2013 IEEE 14th Workshop on Control and Modeling for Power Electronics, COMPEL 2013, art. No. 6626473

11 Roisum, D.R.: The mechanics of winding, TAPPI PRESS, Atlanta, 1994.

[12] Lennon, G.E., Martin, J.R., Anderson, C.D.: Single-ply paperboard tube and method of forming same, US Patent US 5586963, 1996

[13] Sato, H., Shimizu, S.: Method of manufacturing paper tube, European patent EP 0699518 A3, 1996

[14] Rautiainen, P.: Papermaking – part 3, finishing, 2nd edition, Paperija Puu Oy, Helsinki, 2010.

[15] Wagner, M., Roosen, A., Oostra, H., Höppener, R., De Moya, M.: Novel low voltage piezoactuators for high displacements, *J. Electroceram.*, **14**, [3], 231 – 238, (2005).

[16] Scheithauer, U., Slawik, T., Scholl, R., Handke, T., Moritz, T., Baumann, A., Grossmann, H., Michaelis, A.: Spiral winding of ceramic and metallic green tapes, (in German), *Keramische Zeitschrift*, **64**, [1], 35 – 39, (2012).

[17] Götschel, I., Gutbrod, B., Travitzky, N., Roosen, A., Greil, P.: Processing of preceramic paper and ceramic green tape derived multilayer structures, *Adv. Appl.Ceram.*, **112**, 358 – 365, (2013).

[18] EN 623 – 2: Advanced technical ceramics; monolithic ceramics; general and textural properties; part 2: determination of density and porosity, European industry norm, 1993.

[19] EN 843 – 2: Advanced technical ceramics. Mechanical properties of monolithic ceramics at room temperature; part 2: determination of Young's modulus, shear modulus and Poisson's ratio, European industry norm, 2007.

[20] Feilhauer, R.: Method for the determination of the flexural strength of etched and formed aluminium foils, in German, German patent DE3717159A1, 1988.

[21] Roosen, A.: New lamination technique to join ceramic green tapes for the manufacturing of multilayer devices, *J. Eur. Ceram. Soc.*, **21**, 1993 – 1996, (2001).

[22] Dudczig, S., Aneziris, C.G., Dopita, M., Rafaja, D.: Application of oxide coatings for improved steel filtration with the aid of a metal casting simulator, *Adv. Eng. Mater.*, **15,** [12], 1177 – 1187, (2013).

[23] Hasselman, D.P.H.: Thermal stress resistance parameters for brittle refractory ceramics: a compendium, *Am. Ceram. Soc. Bull.*, **49**, 1033 – 1037, (1970).